Coupled Spin Torque Nano-Oscillators: Stability of Synchronization

K. Beauvais, A. Palacios, R. Shaffer, J. Turtle, V. In and P. Longhini

Abstract In this work we explore the use of spin torque nano-oscillators (STNOs) to produce a spintronics voltage oscillator in the microwave range. STNOs are quite small—on the order of 100 nm—and frequency agile. However, experimental results till date have produced power outputs that are too small for practical use. We attempt to increase power output by investigating the dynamics of a system of electrically-coupled STNOs. Transverse Lyapunov exponents are used to quantitatively measure the local stability of synchronized limit cycles. The synchronized solution is found to be stable for a large region of two-parameter space. However, a two-parameter bifurcation diagram reveals a competing out-of-phase solution, causing bistability.

1 Introduction

Spin torque nano-oscillators (STNO) are a ferromagnet-based electronics component. In certain steady states, the magnetic moment precesses causing component resistance to oscillate [12]. Based on this oscillating resistance, an STNO can be utilized as a microwave-range voltage oscillator (see Fig. 1). However, STNOs tested till date have yet to produce adequate power. STNOs need to output at least 1 mW to be applicable [11]. The microwave power generated by an STNO was first measured in 2010 on the order of 1 nW [5]. One solution to increasing power is to electrically couple multiple oscillators. However, in experiments it has been proven that it is difficult to synchronize even two STNOs [8]. Thus, we have begun to study the dynamics of coupled STNOs to determine conditions for synchronization. In this chapter we describe the model in Cartesian coordinates and then project to complex

A. Palacios (✉) · K. Beauvais · R. Shaffer · J. Turtle
Nonlinear Dynamical Systems Group, Department of Mathematics,
San Diego State University, San Diego, CA 92182, USA
e-mail: apalacios@mail.sdsu.edu

V. In · P. Longhini
Space and Naval Warfare Systems Center, Code 2363, 53560 Hull Street,
San Diego, CA 92152-5001, USA

Fig. 1 Series arrayed STNOs
with input current I_{DC} and
output resistance R_c. The
fixed ferromagnetic layer is
green with magnetic moment
M. The free ferromagnetic
layer is *red* and its magnetic
moment is modeled by **m**
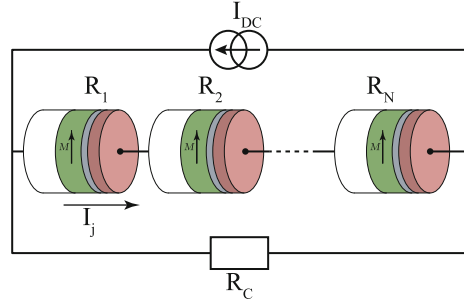
stereographic coordinates. Next, we numerically analyze the local stability of synchronized limit cycles using transverse Lyapunov exponents (TLE). Following TLEs, we investigate global behavior by creating a two-parameter bifurcation diagram.

2   The Model

Magnetization in the free ferromagnetic layer is described by the Landau–Lifshitz equation with Gilbert damping and Slonczewski–Berger spin-torque term (LLGS) [1, 2, 4, 6, 13]

$$\frac{d\mathbf{m}}{dt} = \overbrace{-\gamma \mathbf{m} \times \mathbf{H}_{\text{eff}}}^{\text{precession}} + \overbrace{\lambda \mathbf{m} \times \frac{d\mathbf{m}}{dt}}^{\text{damping}} - \overbrace{\gamma a\, g(P, \mathbf{m} \cdot \mathbf{M})\, \mathbf{m} \times (\mathbf{m} \times \mathbf{M})}^{\text{spin transfer torque}}, \quad (1)$$

where **m** represents the magnetization of the free ferromagnetic layer in Cartesian coordinates, γ is the gyromagnetic ratio, and $\mathbf{H}_{\text{eff}}$ is the effective external field. λ serves as the magnitude of the damping term. In the spin-torque term, a has units Oe and is proportional to the electrical current density [10]. g is a scalar function of the polarization factor P, **m**, and the fixed-layer magnetization direction **M**. To determine the change of field direction with respect to time, we must consider three different classes of torques acting on the field direction **m**: effective external magnetic field $\mathbf{H}_{\text{eff}}$, damping λ, and spin transfer torque. $\mathbf{H}_{\text{eff}}$ is the sum of several factors that can be effectively represented as external fields. The factors that we consider in this fashion are exchange, anisotropy, and demagnetization. The actual external, or applied, field rounds out the sum

$$\mathbf{H}_{\text{eff}} = \mathbf{H}_{\text{exchange}} + \mathbf{H}_{\text{anisotropy}} + \mathbf{H}_{\text{demagnetization}} + \mathbf{H}_{\text{applied}}.$$

We model the free layer as a single particle who's magnetization **m** represents the average of the layer. Thus, there is no exchange with adjacent magnetic moments $\mathbf{H}_{\text{exchange}} = 0$.

Complex Stereographic Projection

A spherical surface can be projected onto a plane by using the complex variable ω and the following relationships:

$$\omega = \frac{m_x + im_y}{1 + m_z} \quad \Rightarrow \quad \mathbf{m} = \begin{bmatrix} \dfrac{\omega + \bar{\omega}}{1 + |\omega|^2} \\ -i\dfrac{(\omega - \bar{\omega})}{1 + |\omega|^2} \\ \dfrac{1 - |\omega|^2}{1 + |\omega|^2} \end{bmatrix}. \tag{2}$$

Here $\bar{\omega}$ is the complex conjugate of ω. This projection maps the sphere's north pole to the origin and the south pole to infinity. Building on [9, 10], we reduce Eq. (1) to the form

$$\begin{aligned}
\dot{\omega} =& \frac{\gamma}{1 - i\lambda}\Big(-a\omega + ih_{a3}\omega + \frac{h_{a2}}{2}(1 + \omega^2) \\
& + im_{\parallel}\kappa \Big[\cos\theta_{\parallel}\omega - \frac{1}{2}\sin\theta_{\parallel}\left(e^{i\phi_{\parallel}} - \omega^2 e^{-i\phi_{\parallel}}\right) \Big] \\
& - \frac{i4\pi S_o}{(1 + |\omega|^2)}\Big[N_3(1 - |\omega|^2)\omega - \frac{N_1}{2}(1 - \omega^2 - |\omega|^2)\omega \\
& \qquad - \frac{N_2}{2}(1 + \omega^2 - |\omega|^2)\omega - \frac{(N_1 - N_2)}{2}\bar{\omega} \Big] \Big),
\end{aligned} \tag{3}$$

where h_{a2} is the magnitude of the applied field in the y-direction and h_{a3} is the magnitudes of the applied field in the z-direction. κ is the anisotropy magnitude who's direction is determined by the spherical-coordinate parameters $\theta_{\parallel}$ and $\phi_{\parallel}$. The anisotropy is scaled by $m_{\parallel} = \mathbf{m} \cdot \mathbf{e}_{\parallel}$ where

$$\mathbf{e}_{\parallel} = \begin{bmatrix} \sin\theta_{\parallel}\cos\phi_{\parallel} \\ \sin\theta_{\parallel}\sin\phi_{\parallel} \\ \cos\theta_{\parallel} \end{bmatrix}.$$

S_0 is the saturation magnetization. Finally, N_1, N_2, and N_3 describe the effective demagnetization field resulting from the shape of the free layer and are constrained by the relationship $N_1 + N_2 + N_3 = 1$. The magnetic moment of an STNO is now described by two dimensions and in a polynomial-like form.

Coupling

Coupling is achieved by modeling a simple electrical circuit with STNOs arrayed in series or parallel. Figure 1 depicts the series configuration. The resistance of each STNO R_i is a function of the angle θ_i between M (fixed layer-green) and $\mathbf{m}$ (free layer-red):

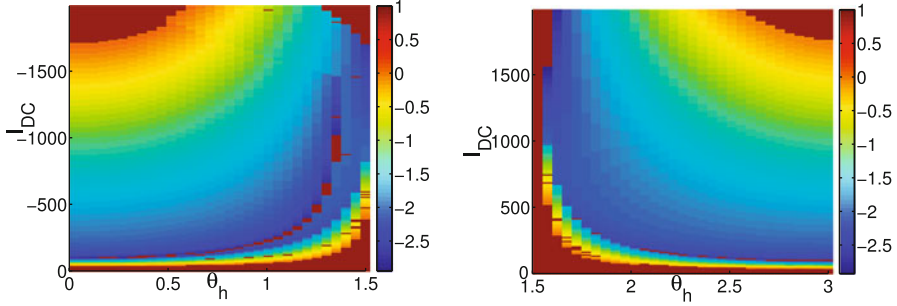$$R_i = R_{0i} - \Delta R_i \cos\theta_i.$$

Fig. 2 Sum of the transverse Lyapunov exponents calculated over two parameters, the electrical current I_{DC} and the angle of the applied field θ_h, with the applied field varying from 0 to $\frac{\pi}{2}$ (*left*) and from $\frac{\pi}{2}$ to π (*right*). Extreme *red* indicates no oscillations

Here, R_0 is the median resistance of an STNO and ΔR is the maximum variance in resistance.

3   Transverse Lyapunov Exponents

Transverse Lyapunov exponents allow us to quantify the local stability of a synchronized orbit [3, 7]. Specifically, TLEs use the linearized system to measure how a small perturbation transverse to the synchronization manifold ($z_s = z_1 = \cdots = z_n$) grows or contracts. Figure 2 depicts the result of numerically calculating TLEs for two serially-coupled and identical STNOs. Here we vary the electrical current I_{DC} with a grid step size $\Delta I_{DC} = 10$ and the applied field angle θ_h with a step size $\Delta\theta_h = 0.05$. Initial conditions are on the synchronization manifold and close to the expected steady state. In this case, the sum of TLEs is a good representation of stability, hence the plot is color coded accordingly. A negative sum indicates stable while a positive sum indicates instability of the synchronized orbit. Additionally, the uniform red color represents areas where no oscillations were detected. These results indicate large regions of parameter space where the synchronized solution is stable. Further, there are distinct boundaries of oscillations that may trace the locus of Hopf bifurcations.

4   Numeric Bifurcation Diagram

We have shown that synchronized oscillations are locally stable for a large parameter space. However, simulations in the same parameter space using random initial conditions show out-of-phase steady-state behaviors [14]. Using the software package XPPAUT, we have created a two-parameter bifurcation diagram (Fig. 3) that
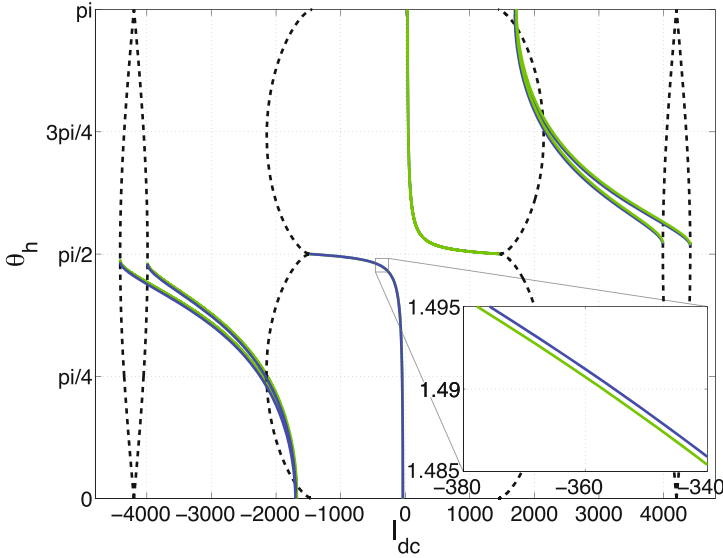
Fig. 3 Two-parameter bifurcation diagram plotting input current I_{DC} v applied field angle θ_h. *Dashed black lines* trace saddle-node bifurcations, while *solid lines* are Hopfs. *Green solid lines* are Hopfs that spawn synchronized limit cycles and *solid blue lines* are Hopfs that spawn out-of-phase oscillations

includes the parameter spaces from Fig. 2. The diagram reveals a number of back-to-back Hopf bifurcations that are consistent with the boundary of oscillations in Fig. 2. Additionally, each pair of back-to-back Hopfs spawns one synchronized and one out-of-phase limit cycle. One-parameter bifurcation diagrams in I_{DC} (θ_h fixed) indicate that the out-of-phase solution is also locally stable for most of the oscillating region. Hence, the region of interest exhibits bistability where we expect the initial conditions to determine synchronized or out-of-phase steady-state behavior.

5   Remarks

The LLGS Eq. (1) is a nonlinear first-order ordinary differential equation confined to the unit sphere $\|\mathbf{m}\|_2 = 1$. We are able to reduce the dimension of the system one third using complex-stereographic coordinates. Not only does this increase the efficiency of numerics but also simplifies integration by fixing the magnitude of $\mathbf{m}$ by the nature of the coordinate system.

The calculation of TLEs in Fig. 2 gives the positive result of stable synchronized oscillations in a large parameter space. However, the TLE measurement is inherently local, and therefore does not necessarily reflect global behavior. Using XPPAUT to create a two-parameter bifurcation diagram, we discover the existence of an out-of-phase limit cycle that is also locally stable. This bistability indicates that

synchronization can only be achieved if the initial conditions fall within the basin of attraction of the synchronized solution.

In future work we are interested in calculating the basins of attraction, but we are also interested in the behavior of the system for many more STNOs. As we increase the number of oscillators N, we expect a nonlinear increase in the number of oscillatory steady states. We intend to leverage the symmetry-group representation of the coupling to predict the type, existence, and stability of out-of-phase oscillations. Combined with the TLE computation, this will allow us to determine if a region exists where the synchronized solution is globally stable.

References

1. Berger, L.: Emission of spin waves by a magnetic multilayer traversed by a current. Phys. Rev. B **54**(13), 9353–9358 (1996). doi:10.1103/PhysRevB.54.9353
2. Bertotti, G., Mayergoyz, I., Serpico, C.: Analytical solutions of Landau-Lifshitz equation for precessional dynamics. Phys. B **343**(1–4), 325–330 (2004)
3. Chitra, R., Kuriakose, V.: Phase effects on synchronization by dynamical relaying in delay-coupled systems. Chaos: Interdisc. J. Nonlinear Sci. **18**(2), 023,129–023, 129 (2008)
4. d'Aquino, M.: Nonlinear magnetization dynamics in thin-films and nanoparticles. Ph.D. thesis, Universitá degli Studi di Napoli Federico II, Naples, Italy (2004)
5. Demidov, V., Urazhdin, S., Demokritov, S.: Direct observation and mapping of spin waves emitted by spin-torque nano-oscillators. Nat. Mater. **9**(12), 984–988 (2010)
6. Gilbert, T.: A phenomenological theory of damping in ferromagnetic materials. IEEE Trans. Magn. **40**(6), 3443–3449 (2004)
7. Krasovskiĭ, N.N.: Stability of Motion: Applications of Lyapunov's Second Method to Differential Systems and Equations with Delay. Stanford University Press (1963)
8. Li, D., Zhou, Y., Zhou, C., Hu, B.: Global attractors and the difficulty of synchronizing serial spin-torque oscillators. Phys. Rev. B **82**(14), 140,407 (2010)
9. Murugesh, S., Lakshmanan, M.: Bifurcation and chaos in spin-valve pillars in a periodic applied magnetic field. Chaos **19**, 043,111 (2009)
10. Murugesh, S., Lakshmanan, M.: Spin-transfer torque induced reversal in magnetic domains. Chaos Solitons Fractals **41**, 2773–2781 (2009)
11. Persson, J., Zhou, Y., Akerman, J.: Phase-locked spin torque oscillators: impact of device variability and time delay. J. Appl. Phys. **101**(9), 09A503 (2007)
12. Slavin, A., Tiberkevich, V.: Nonlinear auto-oscillator theory of microwave generation by spin-polarized current. IEEE Trans. Magn. **45**(4), 1875–1918 (2009)
13. Slonczewski, J.C.: Current-driven excitation of magnetic multilayers. J. Magn. Magn. Mater. **159**(1–2), L1–L7 (1996)
14. Turtle, J;.A.: Numerical exploration of the dynamics of coupled spin torque nano oscillators. M.S. thesis, San Diego State University, San Diego, CA (2012).